JCTC Journal of Chemical Theory and Computation

Article

pubs.acs.org/JCTC

Optimizing Protein–Protein van der Waals Interactions for the AMBER ff9x/ff12 Force Field

Dail E. Chapman,[†] Jonathan K. Steck,[†] and Paul S. Nerenberg*

W. M. Keck Science Department, Claremont McKenna, Pitzer, and Scripps Colleges, Claremont, California 91711-5916, United States

Supporting Information

ABSTRACT: The quality of molecular dynamics (MD) simulations relies heavily on the accuracy of the underlying force field. In recent years, considerable effort has been put into developing more accurate dihedral angle potentials for MD force fields, but relatively little work has focused on the nonbonded parameters, many of which are two decades old. In this work, we assess the accuracy of protein–protein van der Waals interactions in the AMBER ff9x/ff12 force field. Across a test set of 44 neat organic liquids containing the moieties present in proteins, we find root-mean-square (RMS) errors of 1.26 kcal/mol in enthalpy of vaporization and 0.36 g/cm^3 in liquid densities. We then optimize the van der Waals radii and well depths for all of the relevant atom types using these observables, which lowers the RMS errors in enthalpy of vaporization and liquid density of our validation set to 0.59 kcal/mol (53% reduction) and 0.019 g/cm^3 (46% reduction), respectively. Limitations in our parameter optimization were evident for certain atom types, however, and we discuss the implications of these observations for future force field development.

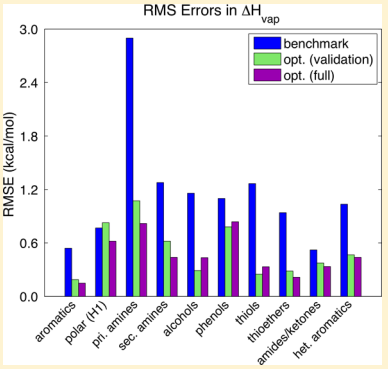

INTRODUCTION

Molecular dynamics (MD) is an important tool for studying the structure, thermodynamics, and interactions of biomolecules because of its unique ability to simulate these systems at atomic resolution over time scales approaching those of biological processes.[1,2] Since the first MD simulations of biomolecules nearly four decades ago, considerable time and effort has been spent on increasing the accuracy of MD force fields to increase both the predictive and analytic capabilities of these simulations. In the cases of the AMBER and CHARMM force fields—arguably the two most widely used biomolecular fixed-charge force fields—the majority of development efforts during the last 15 years have focused on improving the dihedral angle potentials for both proteins[3−8] and nucleic acids,[9−12] leaving the nonbonded parameters (e.g., partial atomic charges or van der Waals radii/well depths) unchanged.

There is a growing realization throughout the simulation community that these improvements are not sufficient to remedy some of the continuing disagreements between MD simulations and experimental measurements of solvation free energies,[13,14] protein folding pathways and transitions,[15−18] native state stability and structure,[19] and the compactness of unfolded states of proteins.[16] In principle, some of these issues could be remedied by the use of polarizable force fields, but there are a number of applications (e.g., cell membranes or intrinsically disordered proteins) for which the decreased computational cost of fixed-charge force fields will be necessary for the foreseeable future. To address these issues, recent development of the GROMOS force field has targeted not only dihedral potentials but also the partial atomic charges and van der Waals parameters.[20−22] Likewise, a new charge model and protein–water van der Waals parameters are being developed for the AMBER ff13 force field.[23] There have also been ad hoc modifications to the nonbonded parameters including polarized protein-specific charges[24] and hydrogen bond-specific charges.[25]

In this work, we assess the accuracy of the protein–protein van der Waals parameters of the AMBER ff9x/ff12 force field. We then introduce new optimized parameters as part of a larger effort to create a new fixed-charge force field parametrized for use with the TIP4P-Ew water model[26] and modern simulation methods (e.g., PME for long-range electrostatics[27]) that leverages much of the existing AMBER force field parametrization infrastructure, including the 6-31G*/RESP charge model. Despite keeping the same charge model, we believe that considerable improvements can be made to this force field and in particular to the van der Waals parameters. Lessons learned from improving this force field may also be useful for the development of next generation fixed-charge force fields.

Previously, we were able to optimize protein–water van der Waals interactions of the AMBER ff9x/ff12 force field and TIP4P-Ew water and subsequently reduce the RMS error in solvation free energies of a set of 47 small molecules from 1.75 to 0.61 kcal/mol.[14] Moreover, we were able to eliminate the systematic undersolvation present in this force field–water model combination. As a consequence of this work, however, we found that the stability of folded proteins was decreased,

Received: July 12, 2013
Published: November 18, 2013

dx.doi.org/10.1021/ct400610x | J. Chem. Theory Comput. 2014, 10, 273−281

prompting an investigation of the strength of protein−protein hydrogen bonds. Adding an additional hydrogen bonding term to the force field did restore much of the stability,[14] but an alternative—or perhaps additional—explanation of this observation is that the protein−protein van der Waals interactions of the AMBER force field are also in need of optimization.

The van der Waals (vdW) parameters currently used by the AMBER ff9x/12 (and GAFF) force fields have been sourced in a variety of different ways. Some parameters were taken from the OPLS force field (derived by matching enthalpies of vaporization and densities of neat organic liquids),[28] while others have been derived by matching ab initio interaction energies or relative solvation free energies.[29,30] It should also be noted that OPLS employs different combining rules for the vdW parameters than AMBER,[28,29] and therefore, it is unclear how OPLS parameters could be adopted to yield identical results in AMBER for any pair of unlike atoms (i.e., atoms of two different types). In short, there has been no single systematic method applied to the derivation of these parameters in the AMBER force fields. This could lead to an imbalance in protein−protein vs protein−water interactions, particularly if the protein−water interactions have been optimized to reproduce solvation free energies.[14] Lastly, to our knowledge these parameters were not derived using two now common aspects of MD simulations: PME for long-range electrostatics and corrections for vdW interactions beyond the cutoff.

With regards to protein−protein interactions, arguably the two most important properties for the protein nonbonded parameters to reproduce are the enthalpies of vaporization and densities of neat liquids of small molecules representing the chemical moieties of amino acid side chains and the peptide backbone.[28] Because these two observables encompass both interaction energies and overall structural distributions, a force field that is able to accurately reproduce them is also likely to accurately reproduce the correct structure and thermodynamics of protein−protein interactions. Additionally, both enthalpy of vaporization and density depend almost entirely on the nonbonded parameters of the force field, and therefore, they are considered a strong test of the quality of these parameters.[31] It is for these reasons that many force fields have tended to place a great emphasis on accurately reproducing these observables.[20,28,29,32,33]

Recent studies by Wang and Hou and Caleman et al. have assessed the accuracy of the GAFF force field (which uses the same vdW parameters as the AMBER ff9x/ff12 force fields for protein atoms) in reproducing enthalpies of vaporization and liquid densities over a wide range of small molecules.[31,34] Wang and Hou also introduced new vdW parameters for three GAFF atom types that were judged to have systematic errors.[31] In this work, we assess the accuracy of the AMBER force field in reproducing these observables over a 44 molecule test set that encompasses all of the chemical moieties (and AMBER atom types) present in protein simulations, with the exception of imidazoles. We find overall RMS errors of 1.26 kcal/mol and 0.036 g/cm^3 in enthalpy of vaporization and liquid density, respectively. Properties of simple alkanes are reproduced with reasonable accuracy. However, several moieties have interactions that are too strong/liquids with densities that are too large, while others have interactions that are too weak/liquids with densities that are too small. By optimizing all of the relevant vdW parameters of the force field, we are able to reduce the overall RMS errors in these observables to 0.59 kcal/mol and 0.019 g/cm^3. Moreover, we are able to substantially reduce the mean signed errors of these observables (i.e., systematic biases) within each category of molecules.

With the parameters derived in this work, we have a force field that can accurately reproduce both protein−protein and protein−water interactions for neutral residues. Before it can be considered complete, however, this force field will require optimization of the nonbonded parameters for charged residues[22,23] and a comprehensive refit of dihedral angle potentials. The parameters derived in this work could also be readily incorporated into GAFF, again with a refit of dihedral angle potentials.

METHODS

Charge Derivation for Small Molecules. Partial atomic charges for all but two of the small molecules in this study were taken from previous work.[14] Charges were derived for bromomethane and m-cresol according to the protocol described in that work. Briefly, the geometry optimization and electrostatic potential calculation of each molecule were conducted at the HF/6-31G* level of theory using GAMESS.[35] Charges were then fit to the potentials from four different molecular orientations using the RESP protocol as implemented in RED III-5.2.[36]

Liquid- and Gas-Phase Simulations. Neat liquid- and gas-phase systems of each molecule were built using the tleap program of AmberTools12.[37] Liquid systems were simulated by filling a cubic box with 512 copies of each molecule, whereas gas-phase systems consisted of just a single molecule. In the liquid phase, periodic boundary conditions were employed with a 9.0 Å cutoff for direct-space nonbonded interactions. In the gas phase, no cutoffs were utilized. Heavy atom−hydrogen bonds were constrained by SHAKE in all simulations, and all simulations were carried out using AMBER 12.[37]

Both gas- and liquid-phase systems first underwent 2000 steps of CG minimization. These systems were then heated to the temperature at which there were known experimental enthalpy of vaporization and density values (Table 1, Supporting Information). The systems were heated to the desired temperature in the NVT ensemble for 20 ps using a Langevin thermostat with a collision frequency of 5.0 ps^{-1}. The liquid simulations were subsequently equilibrated in the NPT ensemble at this temperature for 250 ps using a Berendsen barostat at 1.0 bar with a time constant of 1.0 ps. Production simulations of the liquid systems were conducted in the NPT ensemble for 5 ns using a Berendsen barostat with a time constant of 2.0 ps. Production simulations of the gas-phase systems were conducted for 20 ns. All production simulations used a Langevin thermostat with a collision frequency of 5.0 ps^{-1}. All dynamics simulations were performed with a 2 fs time step, and energy and density data were recorded every 1 ps.

Enthalpy of vaporization values were calculated from the simulation data using

$$\Delta H_{\mathrm{vap}}^{\mathrm{MD}}(T) = U_{\mathrm{gas}}(T) - U_{\mathrm{liquid}}(T) + \frac{1}{2}R\Delta T(3N_{\mathrm{atoms}} - 6 - N_{\mathrm{cons}}) + RT \quad (1)$$

where U_{gas} and U_{liquid} are the potential energies of the gas and liquid phase systems, ΔT is the difference in average simulation temperature between the gas- and liquid-phase systems, N_{atoms} is the number of atoms in the molecule, and N_{cons} is the number of constrained bonds (i.e., constrained heavy atom−H

bonds due to SHAKE).[31] Liquid density values were calculated from AMBER's default output files.

Deviations from experimental enthalpies of vaporization were calculated according to

$$\Delta\Delta H_{vap} = (\Delta H_{vap}^{MD} - W_{pol}) - \Delta H_{vap}^{expt} \quad (2)$$

where W_{pol} is the energetic cost of polarizing the charge distribution of the molecule as it goes from the gas to condensed phase. There have been many methods proposed to incorporate the energetic cost of polarizing the charge distribution of a molecule as it moves from the gas phase to the condensed phase.[23,38−41] To be consistent with prior work on protein−water vdW interactions[14] and observations that simple atom-centered charge models may yield inaccurate higher order multipoles (quadrupole, etc.) for some moieties,[42] we consider only the dipole−dipole polarization cost outlined by Swope et al.[38] While this polarization cost methodology has known limitations, it is—to our knowledge—the only recently developed method that avoids modifications to the charge model, which would break compatibility with the existing infrastructure developed for the AMBER ff9x/ff12 force field.

Deviations from experimental liquid densities were calculated according to

$$\Delta\rho = \rho^{MD} - \rho^{expt} \quad (3)$$

Statistical uncertainties (standard errors of the means) in both of the enthalpies of vaporization and densities were calculated according to

$$SU_i = \frac{\sigma_i}{\sqrt{t_{sim}/2\tau_i}} \quad (4)$$

where σ_i and τ_i are the standard deviation and autocorrelation time of observable i, and t_{sim} is the simulation length.[43] Experimental data are taken from either the CRC Handbook of Chemistry and Physics[44] or ref 34.

Optimization Protocol. We chose 44 small molecules that encompass the chemical moieties of amino acid side chains and the peptide backbone. These 44 small molecules were then categorized by functionality into 11 groups, each containing four molecules. Two molecules from each group were chosen as optimization targets and simulated with varying van der Waals parameters; the other two molecules of the group were used for validation with the optimized van der Waals parameters. Ideally, we would optimize all of the van der Waals parameters simultaneously; however, this is not computationally feasible at present. Therefore, we optimized parameters separately beginning with simple alkanes and eventually progressing to more chemically complicated molecules such as amides or heterocyclic aromatics (see Figure 1 in Nerenberg et al. for the exact order[14]).

The main goal of our optimization process was to minimize the following error function for each category of small molecules

$$E = \frac{1}{N_m}\sum\left[\left(\frac{\Delta\Delta H_{vap}}{\delta\Delta H_{vap}}\right)^2 + \left(\frac{\Delta\rho}{\delta\rho}\right)^2\right] \quad (5)$$

where N_m is the number of experimental measurements, $\Delta\Delta H_{vap}$ and $\Delta\rho$ are the same as in eqs 2 and 3, and $\delta\Delta H_{vap}$ and $\delta\rho$ are predefined error tolerances for the enthalpy of vaporization and liquid density, respectively. This function enables the simultaneous targeting of enthalpy of vaporization and liquid density during the optimization process. The relative "importance" of enthalpy of vaporization versus liquid density is determined by the values of $\delta\Delta H_{vap}$ and $\delta\rho$. Because most of the enthalpies of vaporization in our test set are ∼10 kcal/mol and most of the liquid densities are ∼1 g/cm^3, we found that values of $\delta\Delta H_{vap}$ = 0.30 kcal/mol and $\delta\rho$ = 0.020 g/cm^3 proved to be a reasonable compromise in ensuring that the contributions to the error score from these two observables were approximately equal. Lastly, N_m was equal to 4 for most categories, but was to equal to 3 for two categories (aromatics and heterocyclic aromatics) that lacked liquid density data for one of the optimization molecules.

The AMBER force fields utilize a Lennard−Jones potential for the vdW interactions

$$U_{vdW} = \sum_{i>j}\varepsilon_{ij}[(R_{ij}/r_{ij})^{12} - 2(R_{ij}/r_{ij})^6] \quad (6)$$

where the atomic radius and well depth energy are defined by the Lorentz−Berthelot mixing rules

$$R_{ij} = R_i + R_j,\ \varepsilon_{ij} = \sqrt{\varepsilon_i\varepsilon_j} \quad (7)$$

We introduced optimization coefficients to the vdW parameters in the following way

$$R_i^{opt} = \alpha_{opt}R_i,\ \varepsilon_i^{opt} = \beta_{opt}\varepsilon_i \quad (8)$$

As simulated liquid properties are usually more sensitive to the atomic radius than the energy well depth, the initial grid search for the optimization coefficients ranged from 0.96 to 1.04 for α_{opt} and 0.84−1.16 for β_{opt}. We then selected the α_{opt} and β_{opt} pair that minimized the error E to the benchmark ΔH_{vap} and density values. We then used this α_{opt} and β_{opt} as a starting point for the next grid search. Usually, each category of atom types required 3−4 stages of grid searches of α_{opt} and β_{opt} before reaching a satisfactory error score (usually $E \leq 1$, but sometimes this was not possible). To avoid overfitting of the parameters to the data, we use the same α_{opt} and β_{opt} for both atoms in moieties for which two atom types are involved (e.g., atom types CA and HA for aromatics). This approach is consistent with our prior approach to optimizing protein−water vdW interactions, and as we show in the Results, it still yields considerable improvements.

RESULTS

Benchmark Simulations. Over our full 44 molecule test set, there is an RMS error of 1.26 ± 0.01 kcal/mol and a mean signed error of +0.20 ± 0.01 kcal/mol in the enthalpies of vaporization. Similarly, there is an RMS error of 0.0361 ± 0.0002 g/cm^3 and a mean signed error of +0.0003 ± 0.0003 g/cm^3 in the liquid densities. Detailed results, including statistical uncertainties in these observables, are presented in Table 1 of the Supporting Information. We summarize these data below and in both Figure 1 and Table 1. To avoid cluttering the text, we include the statistical uncertainties in the RMS and mean signed errors of each category only in Table 1. As seen above, however, these uncertainties are generally so small that they can be considered negligible.

From our benchmark results, it is apparent that the existing van der Waals (vdW) parameters for the CT/HC atom types, corresponding to alkane carbon and hydrogen atoms, are quite reasonable (Figure 1). In particular, for the alkanes the RMS errors in enthalpy of vaporization (ΔH_{vap}) and density are 0.24 kcal/mol and 0.014 g/cm^3, respectively (Table 1). The mean

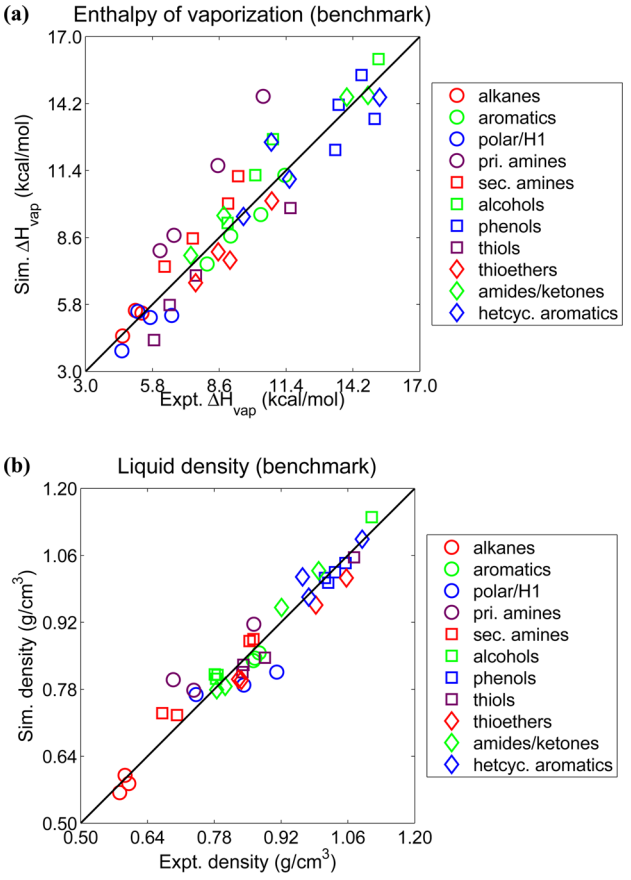

Figure 1. Benchmark data for the AMBER ff9x/ff12 force fields showing simulation vs experiment comparisons of (a) enthalpy of vaporization and (b) liquid density. Methane is not included in (a), and both methane and bromomethane are not included in (b) to enhance the plot details. Data for these molecules are included in Figure 1 of the Supporting Information. Statistical uncertainties in the simulated observables are given in Table1.

signed errors are similarly small: +0.12 kcal/mol and −0.006 g/cm^3 (Table 1). By contrast, we find that the aromatic hydrocarbons (atom types: CA/HA) have interactions that are systematically too weak and densities that are too low, with mean signed errors in ΔH_{vap} and density of −0.49 kcal/mol and −0.020 g/cm^3, respectively (Table 1). These results are in agreement with the prior work of Wang and Hou.[31] Moreover, in previous work, we found that these moieties are systematically undersolvated in TIP4P-Ew water, suggesting the vdW interactions are broadly too weak.[14]

The polar/H1 category is a set of molecules that contain the atom type H1, which corresponds to hydrogen atoms bound to an sp^3 carbon atom that is also bound to an electron-withdrawing heavy atom (e.g., nitrogen or oxygen). This atom type is commonly found, for example, at the Hα position of proteins (because Cα is bonded to N). The molecules we chose for this category have either three or six H1 atoms and only one electron-withdrawing heavy atom, so as to be maximally reflective of the quality of the H1 parameters. Even with newer vdW parameters for some of the other atoms present in these molecules (chlorine[45] and bromine[31]), we find that most of the interactions are too weak and the liquid densities are too low with mean signed errors in ΔH_{vap} and density of −0.52 kcal/mol and −0.038 g/cm^3, resepctively (Table 1). Similarly, in TIP4P-Ew water many of the same molecules were undersolvated, again suggesting vdW interactions that are too weak.[14]

As in our previous work, we split the amines into primary amines (new atom types: NQ/HQ) and secondary amines (atom types: N/H). Here, we find that both types of amines have interactions that are systematically too strong and liquid densities that are too high (Figure 1). In particular, the primary amines have mean signed errors of +2.76 kcal/mol in ΔH_{vap} and +0.067 g/cm^3 in density, while the secondary amines have mean signed errors in these observables of +1.24 kcal/mol and +0.033 g/cm^3 (Table 1). Interestingly, primary amines were the only protein moiety to be oversolvated in TIP4P-Ew water, suggesting that the vdW interactions for these atoms are indeed too strong. Conversely, the secondary amines were *strongly* undersolvated in TIP4P-Ew water.[14] The opposing errors in neat liquid interactions versus aqueous solvation suggest that the charge model may also be deficient for these moieties (see Discussion).

As shown in Figure 1, the interactions of alcohols (atom type: OH) are generally too strong (MSE: +1.00 kcal/mol) and the liquids are too dense (MSE: +0.025 kcal/mol), although they are not as inaccurate as the amines. By contrast, the phenol interactions are slightly too weak (MSE: −0.34 kcal/mol) and the liquids are not quite dense enough (MSE: −0.009 kcal/

Table 1. Root-Mean-Square (RMSE) and Mean Signed (MSE) Errors in Enthalpies of Vaporization and Liquid Densities for All 11 Categories of Small Molecules Considered in This Work[a]

	errors in ΔH_{vap} (kcal/mol)		errors in density (g/cm^3)	
category	RMSE	MSE	RMSE	MSE
alkanes	0.24 (0.006)	+0.12 (0.007)	0.014 (0.0002)	−0.006 (0.0002)
aromatics	0.54 (0.012)	−0.49 (0.012)	0.020 (0.0002)	−0.020 (0.0002)
polar/H1	0.77 (0.005)	−0.52 (0.004)	0.058 (0.0004)	−0.038 (0.0004)
primary amines	2.90 (0.013)	+2.76 (0.012)	0.072 (0.0003)	+0.067 (0.0003)
secondary amines	1.28 (0.013)	+1.24 (0.013)	0.036 (0.0002)	+0.033 (0.0002)
alcohols	1.16 (0.008)	+1.00 (0.008)	0.026 (0.0003)	+0.025 (0.0003)
phenols	1.10 (0.015)	−0.34 (0.017)	0.011 (0.0003)	−0.009 (0.0005)
thiols	1.26 (0.009)	−1.16 (0.010)	0.025 (0.0002)	−0.022 (0.0002)
thioethers	0.94 (0.010)	−0.88 (0.011)	0.038 (0.0002)	−0.037 (0.0002)
amides/ketones	0.52 (0.011)	+0.35 (0.011)	0.023 (0.0002)	+0.009 (0.0002)
heterocyclic aromatics	1.03 (0.007)	+0.08 (0.008)	0.029 (0.0002)	+0.016 (0.0003)

[a]Statistical uncertainties in these errors are shown in parentheses; in many cases—especially for densities—these uncertainties are smaller than the reported significant figures.

dx.doi.org/10.1021/ct400610x | J. Chem. Theory Comput. 2014, 10, 273−281

mol). These data are consistent with previous observations that alcohols are more favorably hydrated than phenols by TIP4P-Ew water.[14] Because of the different behaviors of alcohols and phenols, we introduce a new atom type (OR) for the hydroxyl oxygens of phenol groups. Recent work by Cerutti et al. suggests that an improved charge model may remedy some of the disparity between the hydroxyl groups in these two moieties and eliminate the need for two different atom types, which we explore further in the Discussion.[23]

Sulfur-containing molecules have previously been noted as problematic for fixed-charge force fields,[14,46−48] and here we find that the interactions for both thiols (atom types: SH/HS) and thioethers (atom type: S) are too weak and that the liquid densities are too low (Figure 1). For thiols, the mean signed errors in ΔH_{vap} and density are −1.16 kcal/mol and −0.022 g/cm^3, respectively, while for thioethers, they are −0.88 kcal/mol and −0.037 g/cm^3, respectively (Table 1). Both of these moieties are also undersolvated by TIP4P-Ew water,[14] suggesting that the vdW interactions are indeed too weak.

Finally, the amides/ketones (atom types: C/O) and heterocyclic aromatics (atom type: H4) are generally well balanced (Figure 1 and Table 1), especially considering their chemical complexity. The five-membered pyrrole sticks out among the latter category as having interactions that are too strong (Table 1, Supporting Information), but similar trends were observed for solvation free energies in TIP4P-Ew water.[14] This does, however, imply that many of the other heterocyclic aromatics have interactions that are too weak, in agreement with our observations above regarding purely hydrocarbon aromatics.

Optimization of Protein−Protein van der Waals Interactions. Because the alkanes yielded sufficiently accurate results during the benchmarking phase, we did not attempt to optimize the vdW parameters for the HC/CT atom types. We were able to generate new optimized vdW parameters for all of the other atom types, however, and summarize the results of this optimization graphically in Figures 2 and 3. In these figures, we present both the validation set of only data and the combined optimization set and validation set ("full set") data to demonstrate that they are similar and that our optimization is robust. A detailed set of results is available in Table 2 of the Supporting Information. We show the statistical uncertainties in the RMS and mean signed errors of each category in Figures 2 and 3. As with our benchmark calculations, the uncertainties are negligible in comparison to the errors themselves. The optimized vdW parameters themselves are presented in Table 2, and the optimization coefficients α_{opt} and β_{opt} for each atom type are given in Table 3 of the Supporting Information.

Overall, we were able to reduce the RMS errors in ΔH_{vap} from 1.26 ± 0.01 kcal/mol to 0.59 ± 0.01 kcal/mol (full set: 0.51 ± 0.01 kcal/mol) and the RMS errors in density from 0.0361 ± 0.0002 g/cm^3 to 0.0194 ± 0.0002 g/cm^3 (full set: 0.0186 ± 0.0002 g/cm^3). Moreover, we were able to reduce the magnitude of both RMS and mean signed errors in ΔH_{vap} for *all* categories of molecules in the full set (Figure 2). The only categories for which the full set RMS errors in ΔH_{vap} were greater than 0.60 kcal/mol after optimization were the primary amines and phenols (Figure 2a). Although not quite as dramatic as our improvements in ΔH_{vap} accuracy, we were likewise able to reduce the magnitude of both RMS and mean signed errors in density for every category, with the exception of phenols (Figure 3). The implications of the primary amine and phenol results are discussed in more detail in the Discussion. In the results that follow, the optimized data are taken only from the validation set, although full set data are shown side-by-side with the validation set data in Figures 2 and 3.

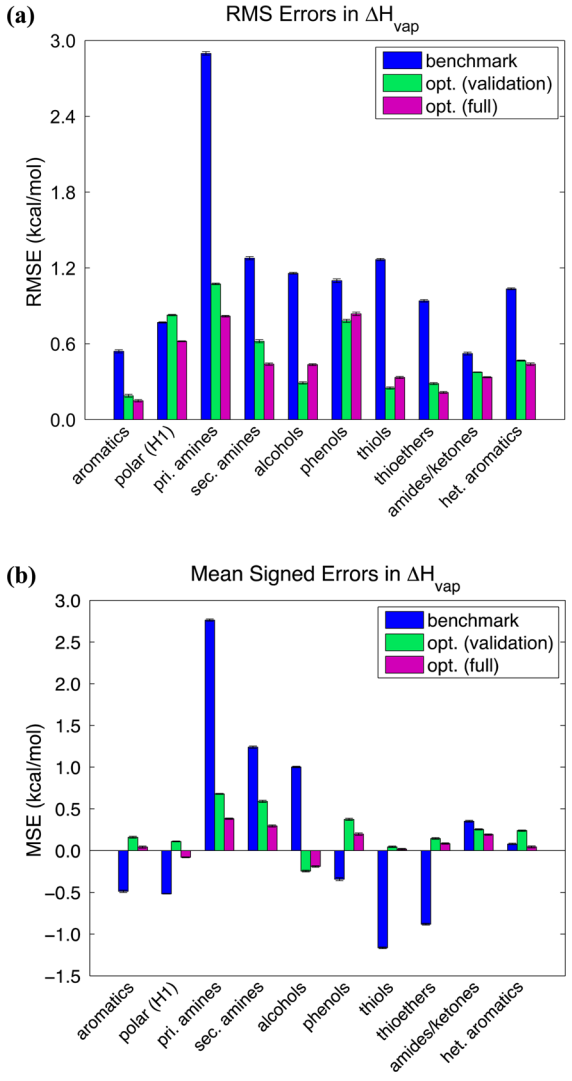

Figure 2. Errors in enthalpies of vaporization for the benchmark AMBER force field (blue) and the optimized vdW parameters (green, validation set; magenta, combined optimization and validation set). Deviations from experimental data are presented as both (a) root-mean-square (RMS) and (b) mean signed errors. Statistical uncertainties in these errors are shown with bars; in general, these uncertainties are insignificant relative to the sizes of the deviations themselves.

For the aromatics, we found that a 1% reduction in radius and 8% increase in well depth of the relevant atom types was able to remedy the disagreement with experiment (Table 2). With these modifications, the mean signed errors in ΔH_{vap} and density decreased from −0.49 kcal/mol to +0.16 kcal/mol (Figure 2b) and −0.020 g/cm^3 to +0.004 g/cm^3 (Figure 3b), respectively. It is noteworthy that our optimization yields a well depth of 0.0929 kcal/mol for the CA atom type, which is in close agreement with the optimized value of 0.0920 kcal/mol determined by Wang and Hou.[31]

The optimization of the polar/H1 molecules is challenging because it is impossible—by definition—to have a molecule with H1-type hydrogen atoms and only alkane or pure

dx.doi.org/10.1021/ct400610x | J. Chem. Theory Comput. 2014, 10, 273−281

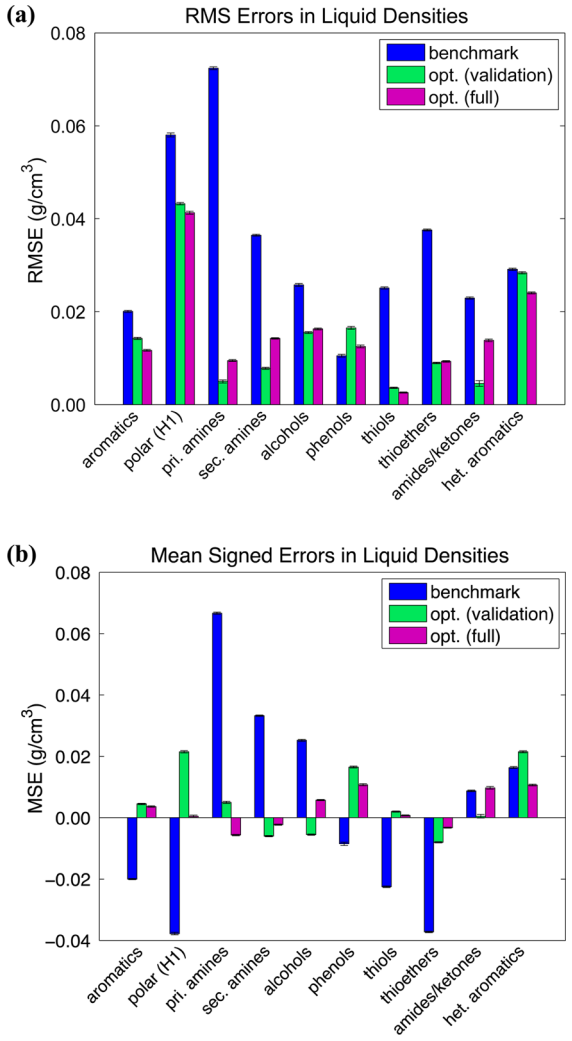

Figure 3. Errors in liquid densities for the benchmark AMBER force field (blue) and the optimized vdW parameters (green, validation set; magenta, combined optimization and validation set). Deviations from experimental data are presented as both (a) root-mean-square (RMS) and (b) mean signed errors. Statistical uncertainties in these errors are shown with bars; in general, these uncertainties are insignificant relative to the sizes of the deviations themselves.

hydrocarbon moieties. In particular the electron-withdrawing heavy atom bonded to the sp^3 carbon will likely have errors associated with its own vdW parameters that contribute to the overall error for a given molecule. As a result, we did not pursue the lowest possible error score in optimizing the vdW parameters for the H1 atom type but rather optimized the parameters until the error score reached ∼1 (i.e., the error was just within our "tolerance" for reasonable accuracy). In the end, we reduced the radius of the H1 atom by 2% and increased the well depth by 30% (Table 2). It is worthwhile to note that these are the same types of changes—smaller radius and larger well depth—that were made to the vdW interactions of H1 atoms with TIP4P-Ew water.[14] As a result of this optimization, we were able to reduce the mean signed errors in ΔH_{vap} and density from −0.52 to 0.11 kcal/mol (Figure 2b) and −0.038 g/cm^3 to 0.022 g/cm^3, respectively (Figure 3b). Of interest to future nucleic acid and small molecule force field development, we found that even after optimization the sole ether-containing molecule (dimethyl ether) had a liquid density that was too high, while the chlorine-containing molecule (chloromethane) had a liquid density that was too low (Table 2, Supporting Information).

Table 2. Ooriginal AMBER ff9x/ff12 and Optimized van der Waals Radii (R_i) and Well Depths (ε_i) for All of the AMBER/GAFF Atom Types Considered in This Work

		original parameters		optimized parameters	
category	atom type(s)	R_i (Å)	ε_i (kcal/mol)	R_i (Å)	ε_i (kcal/mol)
alkanes	HC/hc	1.4870	0.0157	n/a	n/a
	CT/c3	1.9080	0.1094	n/a	n/a
aromatics	HA/ha	1.4590	0.0150	1.4444	0.0162
	CA/ca	1.9080	0.0860	1.8889	0.0929
polar/H1	H1/h1	1.3870	0.0157	1.3593	0.0204
primary amines	HQ/hq	0.6000	0.0157	0.6600	0.0129
	NQ/nq	1.8240	0.1700	2.0064	0.1394
secondary amines	H/hn	0.6000	0.0157	0.6960	0.0129
	N/n3	1.8240	0.1700	2.1158	0.1326
alcohols	OH/oh	1.7210	0.2104	1.7900	0.2420
phenols	OR/or	1.7210	0.2104	1.7382	0.2567
thiols	HS/hs	0.6000	0.0157	0.6240	0.0214
	SH/sh	2.0000	0.2500	2.0800	0.3400
thioethers	S/ss	2.0000	0.2500	2.0000	0.2900
amides/ketones	O/o	1.6612	0.2100	1.4619	0.2352
	C/c	1.9080	0.0860	1.6790	0.0963
heterocyclic aromatics	H4/h4	1.4090	0.0150	1.2399	0.0162

We were able to dramatically reduce both the RMS and mean signed errors in ΔH_{vap} of the primary amines (changes of 2.90 to 1.07 kcal/mol and +2.76 to +0.68 kcal/mol, respectively, as shown in Figure 2), but we note that no further improvement is possible without making the liquid densities excessively low. As is, the mean signed error in density for this moiety was reduced from +0.067 g/cm^3 to +0.005 g/cm^3 (Figure 3b). Likewise, we were able to improve the secondary amines with respect to all metrics. Focusing on just the mean signed errors, these decreased from +1.24 kcal/mol to +0.59 kcal/mol (Figure 2b) and +0.033 g/cm^3 to −0.006 g/cm^3 (Figure 3b) for ΔH_{vap} and density, respectively. For both primary and secondary amines, these improvements were brought about by increases in the vdW radii (10% and 16%, respectively) and decreases in the well depths (18% and 22%, respectively) (Table 2).

Improving the accuracy of the too strong/overly dense alcohols also proved to be straightforward. The mean signed errors in ΔH_{vap} and density decreased from +1.00 kcal/mol to −0.24 kcal/mol and +0.025 g/cm^3 to −0.006 g/cm^3, respectively (Figures 2b and 3b). As with the amines, the densities were decreased by increasing the vdW radius of the hydroxyl oxygen by 4% (the hydroxyl hydrogen has no vdW parameters, as in the TIP3P/TIP4P water models), but the well depth needed to be increased by 15% to maintain the strength of the interactions (Table 2). Although we increased the radius and well depth of the phenol hydroxyl oxygen by 1% and 22%, respectively (Table 2), we found it difficult to improve the accuracy of this moiety in any significant way. In fact, the modest increase in accuracy of ΔH_{vap} (Figure 2) was accompanied by a small decrease in accuracy of density (Figure 3). With different values of $\delta\Delta H_{vap}$ and $\delta\rho$ in our error function, it is likely that the changes would be insignificant with respect to the benchmark data.

The sulfur-containing thiols and thioethers also demonstrated significant improvement from their benchmark results. Specifically, the mean signed errors in ΔH_{vap} improved from −1.16 kcal/mol to +0.04 kcal/mol and −0.88 kcal/mol to +0.14 kcal/mol, respectively (Figure 2). Similarly, the mean signed errors in density improved from −0.022 g/cm^3 to +0.002 g/cm^3 and −0.037 g/cm^3 to −0.008 g/cm^3, respectively (Figure 3). In both cases the vdW well depths of the associated atom types were increased (36% and 16%, respectively), while the thiols also required a modest increase in vdW radii (4%) to prevent the liquid densities from becoming too high with the stronger interactions (Table 2).

The biggest challenge with the amides/ketones was maintaining their relatively good accuracy after modifying the vdW parameters of all of the other atom types found in these moieties (e.g., the amine portion of the amides). As the strength of interactions and densities of the amines were reduced by optimization, we needed to increase the strength of the carbonyl interactions in the amide groups without disrupting the accuracy of "pure" ketone compounds (e.g., propanone). We found that this was possible by reducing the radii of the C and O atoms by 12% and increasing the well depths by 12% (Table 2). One might question the choice of altering the vdW parameters for both the C and O atoms, but we found that this resulted in greater accuracy of both ΔH_{vap} and density as opposed to leaving the C atom parameters equal to those of aromatic carbon atoms, as is currently done in the AMBER force fields.[29] Recent work by Cerutti et al. has shown that modifying only the O vdW parameters is sufficient to improve the accuracy of solvation free energies (and therefore potentially enthalpies of vaporization and densities), but we note that this result has been obtained with a new more strongly polarized charge model.[23]

Lastly, we were successful in improving the accuracy of ΔH_{vap} for the heterocyclic aromatics, as registered by a decrease in RMS error from 1.03 to 0.47 kcal/mol (Figure 2a), but actually made the densities of the validation set slightly less accurate (Figure 3). We ascribe most of the improvement to the changes in the parameters of the aromatic carbon and hydrogen atoms rather than the H4 atom type found in these molecules. Nonetheless, as with the H1 atom type, we note that it was beneficial to reduce the radius and increase the well depth of the H4 atom type (Table 2).

DISCUSSION

The ultimate measure of the accuracy of biomolecular MD force fields is their ability to predict or reproduce experimental data. While MD force fields have clearly improved with time,[49] several studies have identified deficiencies even with the latest force fields.[16,17,19] In general, these force fields seem to be adequate for simulating the native states of stable, well-folded proteins, but the accumulation of inaccuracies in protein−protein and protein−water interactions may have a large effect in simulations of protein folding processes, folded proteins of marginal stability, or intrinsically disordered proteins. Although it is not the subject of this work, the same is likely true of simulations involving nucleic acids, which are generally highly solvent-exposed.

In this work, we investigated the accuracy of protein−protein interactions in the AMBER ff9x/ff12 force field through examining the enthalpies of vaporization and liquid densities of various small molecules containing the moieties found in proteins. By comprehensively optimizing only the van der Waals radii and well depths of the relevant atom types, we were able to significantly improve the accuracy of this force field. Specifically, the overall RMSE of enthalpy of vaporization and liquid density were reduced by 53% and 46%, respectively, to final values of 0.59 kcal/mol and 0.019 g/cm^3. Moreover, we were able to remedy many of the systematic biases that were present in the force field (e.g., the overly strong interactions of amines or overly weak interactions of thiols).

Electrostatic interactions also play a large role in correctly reproducing both of these observables, but we have intentionally left the charge model as is so as to not break compatibility with the existing charge derivation methods for the AMBER ff9x/ff12 and GAFF force fields. Nonetheless, despite keeping the nearly two decade-old 6-31G*/RESP charge model, we were able to achieve what many would regard as sufficient or "chemical" accuracy in these interaction energies by optimization of van der Waals parameters alone.

On the whole, our optimized vdW parameters yielded significant improvements to the force field, but it is instructive to examine the cases where this optimization left us short of the desired accuracy. For example, while we were able to dramatically reduce the RMS and mean signed errors in ΔH_{vap} for the primary amines (Figure 2), our vdW parameter optimization reached a clear limit: we were unable to reduce the RMS error for this moiety below ∼0.8 kcal/mol without the densities of the liquids becoming unacceptably small. It is also noteworthy that we had to create a new pair of atom types for the nitrogen atom and its attached hydrogen atoms (distinct from that of the secondary amines) to reach this level of accuracy. Somewhat more troubling was the lack of substantial improvement in the accuracy of phenol enthalpies of vaporization and densities (Figures 2 and 3), despite the successful optimization of aromatic hydrocarbon atom types and the implementation of a unique atom type for phenol hydroxyl oxygens.

The above data suggest that the errors found in the amines and phenols may be caused not only by inaccurate vdW parameters but also by inaccuracies in the charge model. (This is not to say that the 6-31G*/RESP charge model is perfectly accurate for all of the other moieties—it surely is not—but optimization of the vdW parameters alone is seemingly able to overcome whatever inaccuracies may exist.) It is possible that a more advanced charge model may yield greater accuracy and also obviate the need for a large number of unique atom types/vdW parameters. Hints of such progress have been shown using the IPolQ charge model of the upcoming AMBER ff13 force field, which is able to reproduce solvation free energies of both alcohols and phenols using a single atom type for the hydroxyl oxygens.[23] Whether this charge model is able to yield similar improvements for protein−protein interactions as assessed via enthalpies of vaporization and liquid densities remains to be seen.

A larger question left open by this work is to what extent optimizing only the vdW parameters might affect the accuracy of reproducing other experimental observables. For example, a recent study by Caleman et al. suggests that although current force fields are able to reproduce enthalpies of vaporization and liquid densities reasonably well, there are considerable errors in reproducing diffusion coefficients, static dielectric constants, and various fluctuation quantities.[34] We hope in the future to evaluate the effects of different charge models on other observables to determine which ones might be most accurate in a broader sense, as this may be a crucial step in developing the

next—and perhaps final—generation of fixed-charge force fields. We likewise believe it would be useful to explore if/how force fields might be made more accurate by incorporating experimental data for some of these other observables in the parametrization process.

■ ASSOCIATED CONTENT

Supporting Information

A version of Figure 1 containing data for all 44 molecules, detailed results of the benchmark and optimization/validation simulations, and optimization coefficients (α_{opt} and β_{opt}) for the van der Waals parameters. This material is available free of charge via the Internet at http://pubs.acs.org..

■ AUTHOR INFORMATION

Corresponding Author

*E-mail: psn@kecksci.claremont.edu.

Author Contributions

†Both authors contributed equally to this work.

Notes

The authors declare no competing financial interest.

■ ACKNOWLEDGMENTS

The work reported here used the resources of the National Energy Research Scientific Computing Center, which is supported by the Office of Science of the U.S. Department of Energy under Contract DE-AC02-05CH11231.

■ REFERENCES

(1) Karplus, M.; McCammon, J. A. *Nat. Struct. Biol.* **2002**, *9*, 646−652.
(2) Dror, R. O.; Dirks, R. M.; Grossman, J. P.; Xu, H.; Shaw, D. E. *Annu. Rev. Biophys.* **2012**, *41*, 429−452.
(3) Hornak, V.; Abel, R.; Okur, A.; Strockbine, B.; Roitberg, A.; Simmerling, C. *Proteins* **2006**, *65*, 712−725.
(4) Best, R. B.; Hummer, G. *J. Phys. Chem. B* **2009**, *113*, 9004−9015.
(5) Best, R. B.; Zhu, X.; Shim, J.; Lopes, P. E. M.; Mittal, J.; Feig, M.; Mackerell, A. D. *J. Chem. Theory Comput.* **2012**, *8*, 3257−3273.
(6) Nerenberg, P. S.; Head-Gordon, T. *J. Chem. Theory Comput.* **2011**, *7*, 1220−1230.
(7) Lindorff-Larsen, K.; Piana, S.; Palmo, K.; Maragakis, P.; Klepeis, J. L.; Dror, R. O.; Shaw, D. E. *Proteins* **2010**, *78*, 1950−1958.
(8) Sorin, E. J.; Pande, V. S. *Biophys. J.* **2005**, *88*, 2472−2493.
(9) Hart, K.; Foloppe, N.; Baker, C. M.; Denning, E. J.; Nilsson, L.; Mackerell, A. D. *J. Chem. Theory Comput.* **2012**, *8*, 348−362.
(10) Zgarbová, M.; Luque, F.; Šponer, J.; Cheatham, T. E.; Otyepka, M.; Jurečka, P. *J. Chem. Theory Comput.* **2013**, *9*, 2339−2354.
(11) Zgarbová, M.; Otyepka, M.; Sponer, J.; Mládek, A.; Banáš, P.; Cheatham, T. E.; Jurečka, P. *J. Chem. Theory Comput.* **2011**, *7*, 2886−2902.
(12) Pérez, A.; Marchán, I.; Svozil, D.; Sponer, J.; Cheatham, T. E.; Laughton, C. A.; Orozco, M. *Biophys. J.* **2007**, *92*, 3817−3829.
(13) Mobley, D. L.; Bayly, C. I.; Cooper, M. D.; Shirts, M. R.; Dill, K. A. *J. Chem. Theory Comput.* **2009**, *5*, 350−358.
(14) Nerenberg, P. S.; Jo, B.; So, C.; Tripathy, A.; Head-Gordon, T. *J. Phys. Chem. B* **2012**, *116*, 4524−4534.
(15) Lindorff-Larsen, K.; Maragakis, P.; Piana, S.; Eastwood, M. P.; Dror, R. O.; Shaw, D. E. *PLoS ONE* **2012**, *7*, e32131.
(16) Best, R. B.; Mittal, J. *Proteins* **2011**, *79*, 1318−1328.
(17) Best, R. B.; Mittal, J.; Feig, M.; Mackerell, A. D. *Biophys. J.* **2012**, *103*, 1045−1051.
(18) Best, R. B. *Curr. Opin. Struct. Biol.* **2012**, *22*, 52−61.
(19) Raval, A.; Piana, S.; Eastwood, M. P.; Dror, R. O.; Shaw, D. E. *Proteins* **2012**, *80*, 2071−2079.
(20) Horta, B. A. C.; Fuchs, P. F. J.; Van Gunsteren, W. F.; Hünenberger, P. H. *J. Chem. Theory Comput.* **2011**, *7*, 1016−1031.
(21) Schmid, N.; Eichenberger, A. P.; Choutko, A.; Riniker, S.; Winger, M.; Mark, A. E.; Van Gunsteren, W. F. *Eur. Biophys. J.* **2011**, *40*, 843−856.
(22) Reif, M. M.; Hünenberger, P. H.; Oostenbrink, C. *J. Chem. Theory Comput.* **2012**, *8*, 3705−3723.
(23) Cerutti, D. S.; Rice, J. E.; Swope, W. C.; Case, D. A. *J. Phys. Chem. B* **2013**, *117*, 2328−2338.
(24) Duan, L. L.; Mei, Y.; Zhang, Q. G.; Zhang, J. Z. H. *J. Chem. Phys.* **2009**, *130*, 115102.
(25) Duan, L. L.; Gao, Y.; Mei, Y.; Zhang, Q. G.; Tang, B.; Zhang, J. Z. H. *J. Phys. Chem. B* **2012**, *116*, 3430−3435.
(26) Horn, H. W.; Swope, W. C.; Pitera, J. W.; Madura, J. D.; Dick, T. J.; Hura, G. L.; Head-Gordon, T. *J. Chem. Phys.* **2004**, *120*, 9665−9678.
(27) Darden, T.; York, D.; Pedersen, L. *J. Chem. Phys.* **1993**, *98*, 10089−10092.
(28) Jorgensen, W. L.; Tirado-Rives, J. *J. Am. Chem. Soc.* **1988**, *110*, 1657−1666.
(29) Cornell, W. D.; Cieplak, P.; Bayly, C. I.; Gould, I. R.; Merz, K. M.; Ferguson, D. M.; Spellmeyer, D. C.; Fox, T.; Caldwell, J. W.; Kollman, P. A. *J. Am. Chem. Soc.* **1995**, *117*, 5179−5197.
(30) Veenstra, D. L.; Ferguson, D. M.; Kollman, P. A. *J. Comput. Chem.* **1992**, *13*, 971−978.
(31) Wang, J.; Hou, T. *J. Chem. Theory Comput.* **2011**, *7*, 2151−2165.
(32) Jorgensen, W. L.; Maxwell, D. S.; Tirado-Rives, J. *J. Am. Chem. Soc.* **1996**, *118*, 11225−11236.
(33) Oostenbrink, C.; Villa, A.; Mark, A. E.; Van Gunsteren, W. F. *J. Comput. Chem.* **2004**, *25*, 1656−1676.
(34) Caleman, C.; van Maaren, P. J.; Hong, M.; Hub, J. S.; Costa, L. T.; van der Spoel, D. *J. Chem. Theory Comput.* **2012**, *8*, 61−74.
(35) Schmidt, M. W.; Baldridge, K. K.; Boatz, J. A.; Elbert, S. T.; Gordon, M. S.; Jensen, J. H.; Koseki, S.; Matsunaga, N.; Nguyen, K. A.; Su, S. J.; Windus, T. L.; Dupuis, M.; Montgomery, J. A. *J. Comput. Chem.* **1993**, *14*, 1347−1363.
(36) Dupradeau, F.-Y.; Pigache, A.; Zaffran, T.; Savineau, C.; Lelong, R.; Grivel, N.; Lelong, D.; Rosanski, W.; Cieplak, P. *Phys. Chem. Chem. Phys.* **2010**, *12*, 7821−7839.
(37) Case, D. A.; Darden, T. A.; Cheatham, T. E.; Simmerling, C. L.; Wang, J.; Duke, R. E.; Luo, R.; Walker, R. C.; Zhang, W.; Merz, K. M.; Roberts, B.; Hayik, S.; Roitberg, A.; Seabra, G.; Swails, J.; Götz, A. W.; Kolossváry, I.; Wong, K. F.; Paesani, F.; Vanicek, J.; Wolf, R. M.; Liu, J.; Wu, X.; Brozell, S. R.; Steinbrecher, T.; Gohlke, H.; Cai, Q.; Ye, X.; Hsieh, M.-J.; Cui, G.; Roe, D. R.; Mathews, D. H.; Seetin, M. G.; Salomon-Ferrer, R.; Sagui, C.; Babin, V.; Luchko, T.; Gusarov, S.; Kovalenko, A.; Kollman, P. A. *AMBER 12*, 2012.
(38) Swope, W. C.; Horn, H. W.; Rice, J. E. *J. Phys. Chem. B* **2010**, *114*, 8621−8630.
(39) Karamertzanis, P. G.; Raiteri, P.; Galindo, A. *J. Chem. Theory Comput.* **2010**, *6*, 1590−1607.
(40) Leontyev, I.; Stuchebrukhov, A. *J. Chem. Phys.* **2009**, *130*, 085102.
(41) Berendsen, H. J. C.; Grigera, J. R.; Straatsma, T. P. *J. Phys. Chem.* **1987**, *91*, 6269−6271.
(42) Swope, W. C.; Horn, H. W.; Rice, J. E. *J. Phys. Chem. B* **2010**, *114*, 8631−8645.
(43) Straatsma, T. P.; Berendsen, H. J. C.; Stam, A. J. *Mol. Phys.* **1986**, *57*, 89−95.
(44) *CRC Handbook of Chemistry and Physics*, 92nd ed.; Haynes, W. M., Ed.; CRC Press/Taylor and Francis: Boca Raton, FL, 2011.
(45) Fox, T.; Kollman, P. A. *J. Phys. Chem. B* **1998**, *102*, 8070−8079.
(46) Kaminski, G. A.; Friesner, R. A.; Tirado-Rives, J.; Jorgensen, W. L. *J. Phys. Chem. B* **2001**, *105*, 6474−6487.
(47) Price, D. J.; Brooks, C. L. *J. Comput. Chem.* **2005**, *26*, 1529−1541.
(48) Mobley, D. L.; Bayly, C. I.; Cooper, M. D.; Dill, K. A. *J. Phys. Chem. B* **2009**, *113*, 4533−4537.

(49) Beauchamp, K. A.; Lin, Y.-S.; Das, R.; Pande, V. S. *J. Chem. Theory Comput.* **2012**, *8*, 1409−1414.